

Associations of White Matter Integrity and Cortical Thickness in Patients With Schizophrenia and Healthy Controls

Stefan Ehrlich^{*1-3}, Daniel Geisler³, Anastasia Yendiki¹, Patricia Panneck¹, Veit Roessner³, Vince D. Calhoun^{4,5}, Vincent A. Magnotta⁶, Randy L. Gollub^{1,2}, and Tonya White⁷⁻⁹

¹MGH/MIT/HMS Martinos Center for Biomedical Imaging, Massachusetts General Hospital, Charlestown, MA; ²Department of Psychiatry, Harvard Medical School, Massachusetts General Hospital, Boston, MA; ³Department of Child and Adolescent Psychiatry, University Hospital Carl Gustav Carus, Dresden University of Technology, Dresden, Germany; ⁴The Mind Research Network, Albuquerque, NM; ⁵Department of Electrical and Computer Engineering, University of New Mexico, Albuquerque, NM; ⁶Department of Radiology, University of Iowa, Iowa City, IA; ⁷Department of Psychiatry and the Center for Magnetic Resonance Research, University of Minnesota, Minneapolis, MN; ⁸Department of Child and Adolescent Psychiatry, Erasmus Medical Centre, Rotterdam, The Netherlands; ⁹Department of Radiology, Erasmus Medical Centre, Rotterdam, The Netherlands

*To whom correspondence should be addressed; Department of Child and Adolescent Psychiatry, Translational Developmental Neuroscience Section, Dresden University of Technology, University Hospital Carl Gustav Carus, Fetscherstraße 74, 01307 Dresden, Germany; tel: +49 (0)351-458-2244, fax: +49 (0)351-458-5754, e-mail: transden.lab@uniklinikum-dresden.de

Typical brain development includes coordinated changes in both white matter (WM) integrity and cortical thickness (CT). These processes have been shown to be disrupted in schizophrenia, which is characterized by abnormalities in WM microstructure and by reduced CT. The aim of this study was to identify patterns of association between WM markers and cortex-wide CT in healthy controls (HCs) and patients with schizophrenia (SCZ). Using diffusion tensor imaging and structural magnetic resonance imaging data of the Mind Clinical Imaging Consortium study (130 HC and 111 SCZ), we tested for associations between (a) fractional anisotropy in selected manually labeled WM pathways (corpus callosum, anterior thalamic radiation, and superior longitudinal fasciculus) and CT, and (b) the number of lesion-like WM regions (“potholes”) and CT. In HC, but not SCZ, we found highly significant negative associations between WM integrity and CT in several pathways, including frontal, temporal, and occipital brain regions. Conversely, in SCZ the number of WM potholes correlated with reduced CT in the left lateral temporal gyrus, left fusiform, and left lateral occipital brain area. Taken together, we found differential patterns of association between WM integrity and CT in HC and SCZ. Although the pattern in HC can be explained from a developmental perspective, the reduced gray matter CT in SCZ patients might be the result of focal but spatially heterogeneous disruptions of WM integrity.

Key words: cortical thickness/fractional anisotropy/structural MRI/DTI/schizophrenia

Introduction

High-resolution structural MRI (sMRI) and diffusion tensor imaging (DTI) are 2 commonly used MRI methods to explore the underlying neurobiology of schizophrenia (SCZ). These approaches capture different properties of the brain that often have been used in isolation, but studies combining these techniques are beginning to emerge.¹⁻³ Although sMRI provides reliable measures of brain structure, DTI provides measures of tissue microstructure.⁴ One important measure obtained from sMRI is cortical thickness (CT), which is defined as the distance between the gray matter (GM)/white matter (WM) interface and the outer rim of gray matter. DTI, on the other hand, taps into diffusion properties of water in the brain.^{5,6} Because neuronal fibers generally course together in the same direction, DTI is well suited to measure WM microstructure. One common measure extracted from DTI is fractional anisotropy (FA), which is a rotationally invariant measure of water diffusion in the brain.⁷ Higher FA implies greater diffusion in one direction, such as occurs in WM tracts as water flows more freely along the axons compared with through the cell wall. Alternatively, lower FA implies water diffusion equally in all directions, such as diffusion in cerebral spinal fluid.

DTI has demonstrated WM abnormalities in individuals at high risk for psychosis and in first-episode, medication-naïve, and patients with chronic SCZ. These studies provide strong evidence for a primary role of WM abnormalities in the pathogenesis of this burdensome disorder.⁸⁻¹⁰ Although there is considerable heterogeneity

in the spatial localization of WM abnormalities,¹¹ recent meta-analyses show that deep (left) frontal and temporal WM regions appear to be more commonly affected.^{8,12,13}

The underlying affected WM tracts include the anterior thalamic radiation (ATR), corpus callosum (CC), and the superior longitudinal fasciculus (SLF). Fibers of the ATR connect the anterior and medial thalamic nuclei and the prefrontal cortex and are thought to be integral to the pathophysiology of SCZ.^{14,15} The CC is the largest WM fiber bundle and has been suggested to play a role in abnormal hemispheric specialization and lateralization in SCZ.¹⁶ The SLF connects the temporal, parietal, and frontal regions and plays an important role in working memory,^{17,18} which is typically impaired in SCZ.^{19,20}

In addition to DTI, sMRI studies also show regional GM changes, most notably reductions of the volume in the medial temporal lobe and ventricular enlargement.^{21–24} More recently, sMRI studies have shown widespread CT reductions in frontal, temporal, and parietal regions in patients with SCZ.^{25–28} Furthermore, CT is highly heritable^{25,29,30} and has been suggested as a promising endophenotype for SCZ.

According to mechanical models of brain development, variations in CT are also thought to be modulated by axonal tension exerted between linked areas.^{31,32} Consequently, the development of WM circuitry and CT should be closely interrelated. Early sMRI studies have reported global increases in WM volume and specific increases in WM density from childhood, through adolescence, and into adulthood.^{2,33,34} Subsequently, voxel-based DTI studies have demonstrated significant increases in FA from childhood to adulthood,³⁵ suggestive of increasing myelination, fiber packing density, fiber coherence, or decreased axon diameter.³⁶ Similarly, GM volumes first increase during early childhood and start to decrease thereafter.³³ This is due to a considerable thinning of the cortex that occurs in children and continues throughout adolescence^{37,38} and even beyond, during adulthood.³⁹ Thus, both CT and FA appear to show parallel changes, but the relationship between these 2 measures and their association with SCZ is yet unknown.

Thus, given the wealth of evidence for abnormalities of WM integrity and GM thickness in SCZ, this study aimed to investigate whether WM characteristics in specific WM tracts and circumscribed disruptions of WM microstructure is related to alterations in GM thickness. Because it is almost impossible to accurately determine where exactly WM tracts connect to cortical neurons using MRI, we modeled associations across the entire cortical surface. On the level of DTI, we used 2 distinct approaches to test different patterns of WM abnormalities. Both approaches were based on the assumption that WM aberrations do not necessarily occur in spatially overlapping regions across individuals. Instead, diffuse WM abnormalities (with slight decreases in FA) might occur at different locations along the same WM tract or might be present as focal abnormalities with dramatic decreases (ie,

a 2 SD drop in FA in at least 50 contiguous voxels) in FA in spatially distinct brain regions.⁴⁰ There is no evidence that these lesion-like WM abnormalities, referred to as “potholes,” arise during normal development.⁴¹

Methods

Participants

The Mind Clinical Imaging Consortium (MCIC) study of SCZ^{42,43} obtained sMRI and functional MRI (fMRI) scans on a total of 328 subjects from 4 participating sites: Massachusetts General Hospital in Boston (MGH), University of Iowa (UI), University of Minnesota (UMN), and University of New Mexico (UNM). The institutional review boards (IRBs) at each of the 4 sites approved the study protocol. After complete description of the study to the participants, written informed consent was obtained from each participant. The patient group (SCZ) included subjects with a Diagnostic and Statistical Manual of Mental Disorders IV (DSM-IV) diagnosis of SCZ, established through administration of structured clinical interviews (see below), and reviewed case files by trained clinicians (who completed 2 days of in-person training and testing using videotaped training materials with “gold standard ratings” to establish a cross-site, interrater reliability >85%). Healthy controls (HCs) were included if they had no history of a medical or Axis I psychiatric diagnosis. All participants were required to be at least 18 years of age and no older than 60, and to be fluent in English. Participants were excluded if they had a history of neurologic disease, psychiatric disease other than SCZ, history of a head injury, history of substance abuse or dependence within the past month, severe or disabling medical conditions, contraindication to MR scanning or intelligence quotient <70 (based on the reading subtest from the Wide Range Achievement Test [WRAT-III]).

The final sample with complete and high-quality sMRI and DTI data comprised 136 HC participants and 118 patients with SCZ.

Clinical Measures

All study participants underwent an extensive clinical diagnostic assessment that included either the Structured Clinical Interview for DSM-IV (SCID), Patient Edition (I/P)/Non-patient Edition (I/NP)⁴⁴ or the Comprehensive Assessment of Symptoms and History (CASH,⁴⁵ see also [table 1](#) and ref. ⁴²). Premorbid cognitive achievement was estimated by the WRAT-III⁴⁶; parental socioeconomic status (SES) was determined using the Hollingshead index⁴⁷ and handedness was determined using the Annett Scale of Hand Preference.⁴⁸ Severity of positive and negative symptoms was rated using the Scale for the Assessment of Positive Symptoms (SAPS) and the Scale for the Assessment of Negative Symptoms (SANS).^{49,50}

Table 1. Demographics and Number of Potholes per Acquisition Site and Diagnostic Group

		<i>n</i>	Sex		Age		WRAT-IIIRT		Parental SES		Handedness		Number of Potholes	
			F	F	Mean	SD	Mean	SD	Mean	SD	Mean	SD	Mean	SD
			<i>n</i>	%										
MGH	HC	23	9	39	40 ^a	10	51.91	3.95	3.04 ^a	0.98	1.04	2.93	0.76 ^a	1.30
	SCZ	34	9	26	37 ^a	10	46.25	6.61	3.13 ^a	0.94	1.06	3.09	13.72 ^a	13.28
UI	HC	51	28	55	31 ^a	10	50.24	4.27	2.90	0.46	0.47	2.03	3.75 ^a	3.55
	SCZ	19	4	21	32 ^a	10	49.11	4.84	2.47	0.70	1.26	3.78	8.63 ^a	5.60
UMN	HC	22	10	45	29 ^a	9	50.86	3.68	2.23 ^a	0.75	0.77	2.16	3.14 ^a	3.40
	SCZ	27	8	30	31 ^a	10	46.04	6.57	2.67 ^a	0.92	1.54	3.01	13.63 ^a	10.93
UNM	HC	40	7	18	29 ^a	12	49.90	4.77	2.40	0.84	0.85	2.06	12.35 ^a	12.22
	SCZ	38	8	21	33 ^a	13	47.58	5.88	3.03	1.23	0.86	2.29	26.03 ^a	12.90
Total	HC	136	54	40	31	11	50.52 ^b	4.30	2.67	0.79	0.73	2.22	5.90 ^b	8.46
	SCZ	118	29	25	34	11	47.11 ^b	6.13	2.88	1.02	1.14	2.94	17.10 ^b	13.29

Note: WRAT-IIIRT, reading subtest of the Wide Range Achievement Test-III; SES, socioeconomic status; handedness, Annett Handedness Scale; MGH, Massachusetts General Hospital; UI, University of Iowa; UMN, University of Minnesota; UNM, University of New Mexico; SCZ, patients with schizophrenia; HC, healthy controls. A series of ANOVA models were performed to detect significant differences of age, WRAT-IIIRT Score, parental SES, handedness, and gender between acquisition sites and diagnostic groups.

^aSignificantly different between acquisition sites on the basis of a linear regression with subsequent Scheffé post hoc tests ($P < .05$).

^bSignificantly different between SCZ and HC ($P < .05$).

Antipsychotic history was collected as part of the psychiatric assessment using the PSYCH instrument,⁵¹ and cumulative and current antipsychotic exposure was calculated using the chlorpromazine (CPZ) conversion factors (see online [supplementary material 1.1](#)).

Structural Image Acquisition

Structural MRI data were acquired with either a Siemen's 1.5-Tesla (MGH, UI, and UNM) or a Siemen's 3-Tesla (UMN) MR scanners. The T_1 -weighted structural brain scans at each of the 4 sites were acquired with an in-plane resolution of 0.625×0.625 mm, a slice thickness of 1.5 mm, and a flip angle of 7 degrees. MGH and UNM used a Siemen's 1.5-Tesla scanner with repetition time (TR) = 12, echo time (TE) = 4.76, and number of excitations (NEX) = 1. UI used a GE 1.5-Tesla Genesis Signa scanner with TR = 20, TE = 6, and NEX = 3. UMN used a Siemen's 3-Tesla scanner with TR = 2530, inverse time (TI) = 1100, TE = 3.79, and NEX = 1.

All DTI images were acquired at each site with a 2 mm isotropic resolution. MGH used a Siemens Sonata 1.5-Tesla scanner with TR = 8900, TE = 80, B values of 0 and 700, NEX = 1, and 60 directions. UI used a Siemens TRIO 3-Tesla scanner with TR = 9500, TE = 90, B values of 0 and 1000, NEX = 4 and 6 directions. UNM used a Siemens Sonata 1.5-Tesla scanner with TR = 9800, TE = 86, B values of 0 and 1000, NEX = 4 and 12 directions. UMN used a Siemens TRIO 3-Tesla scanner with TR = 10 500, TE = 86, B values of 0 and 1000, NEX = 2 and 12 directions.

Cross-site MRI acquisition calibration and reliability were established in a preceding study using human phantoms, following guidelines developed by the biomedical informatics research network (BIRN) test bed for morphometry.^{52,53}

Structural Image Data Processing

Structural MRI data from 3 consecutive volumes were registered, motion corrected, averaged, and analyzed in an automated manner with atlas-based FreeSurfer software suite (<http://surfer.nmr.mgh.harvard.edu>, Version 4.0.1). This process included volumetric segmentation, cortical surface reconstruction (see also online [supplementary material 1.2](#)⁵⁴⁻⁵⁸), and the estimation of total intracranial volume (ICV).⁵⁹ The applied method has been thoroughly evaluated and previously applied in a wide variety of settings, including multicenter studies.

Tract-Based Diffusion Data Processing

For the tract-specific FA values, we limited our analysis to participants of the MGH site due to their superior DTI acquisition protocol. We used a standard method, available in FMRIB Software Library (FSL) (<http://www.fmrib.ox.ac.uk/fsl>), for mitigating distortions induced by eddy currents and motion by registering the diffusion-weighted images to the $b = 0$ images after spatial normalization of the diffusion-weighted images (using the reconstructed high-resolution T_1 -weighted images and an intrasubject affine registration method that maximizes the intensity contrast gradient of the image across

the gray/white boundary).⁶⁰ The eddy current-corrected diffusion images were then processed in Trackvis (<http://trackvis.org>). Deterministic tensor streamline tractography was applied to the whole brain using the FACT method.⁶¹ Manual labeling of the whole-brain streamline solutions was then performed in Trackvis to isolate the tracts belonging to the WM pathway of interest (for more details, please refer to ref.⁶²). Specifically, we followed the protocol described by Wakana et al⁶³ to label the forceps major (CC-fmj) and minor (CC-fmi) of the corpus callosum, the anterior thalamic radiation (ATR) in both hemispheres (rh = right hemisphere and lh = left hemisphere) and the parietofrontal part of the rh/lh SLF (see also online [supplementary figures 1 and 4](#)). FA values were averaged over all the voxels that intersected with the streamlines of each tract.

No-Overlap Requirement Spatial Analyses of Diffusion Data

An overview of the no-overlap requirement spatial analyses (NORSA) or the “pothole” approach is available elsewhere.⁴⁰ Briefly, using spatially normalized images, a mean and SD images were created using all the individual FA images from the control group within each of the 4 sites. These mean and SD images were then used to transform all images into z -images for both the patients and controls. The z -transformation is performed within each site, using the mean and SDs for the controls at that site. For each generated z -image, an algorithm searches for contiguous clusters of voxels that drop below a set z -score, which was set at $z = -2$. To reduce the likelihood that the potholes are merely a chance finding the minimum volume of each pothole was set to 50 voxels (see also ref.⁴¹) and the number of potholes in each participant was used for further analyses.

Statistical Analyses

Group differences of basic demographics were examined with ANOVA models, Student t tests, and chi-square tests using SPSS 17.0.

Entire cortex vertex-wise analyses of CT were performed with FreeSurfer (for details please refer to online [supplementary material 1.2](#)). Statistical maps were generated by computing general linear models (GLM) of the effects of each predictor variable on CT at each vertex. Because of known confounding effects and in line with similar studies, we included age, gender, and acquisition site (for the pothole analysis) into the models as control variables.^{25,27,64–67} All CT results were corrected for multiple comparisons using a Monte-Carlo simulation (uncorrected results not reported). This procedure includes the following steps: (1) The initial vertex-wise threshold was set to $P = .05$ to form spatially contiguous areas of association (referred to as “cluster”). (2) The likelihood that a finding (cluster) of this size and magnitude (difference

in thickness as specified by the VWT) would appear by chance, ie, when using repeated random sampling, was tested using Monte-Carlo simulation with 10 000 repeats. This results in a cluster-wise probability (CWP), which is reported as P -values throughout the results section. In addition, for our tract-specific analysis, CWP values were corrected for the number of tested WM tracts (CC-fmj, CC-fmi, rh/lh ATR, and rh/lh SLF = 6 tracts) in our main analysis using the Bonferroni method.

Furthermore, we performed additional analyses to control for possibly confounding effects caused by handedness or cumulative antipsychotic exposure (see online [supplementary material 2.2](#)).

Results

Sample Characteristics

Patients with SCZ and HCs did not differ in age, parental SES, and handedness score ([table 1](#)). Patients had a significantly lower estimated premorbid cognitive function than controls ([table 1](#)). The clinical characteristics of the SCZ cohort are listed by acquisition site in online [supplementary table 1](#).

Reduced White Matter Integrity and Cortical Thickness in Schizophrenia

As expected, patients with SCZ had reduced FA in the CC-fmj, lh-ATR, and rh-ATR when compared with HCs (see online [supplementary table 2](#)). They also had a significantly greater number of potholes (for the full sample: $T = -7.9$, $df = 237$, $P < .001$; see also [table 1](#)).

In accordance with previous studies^{25,27,66} and using the same technique, entire cortex vertex-wise statistics revealed widespread bilateral thickness reductions in SCZ patients, most pronouncedly in the frontal lobe, temporal cortex, inferior parietal lobe, and occipital cortex (see online [supplementary figure 2](#)). There were no regions where CT was increased when compared with HCs.

Significant Associations Between Tract-Specific Fractional Anisotropy and Cortical Thickness

Associations between CT at each vertex and tract-specific FA were tested separately in the groups of MGH schizophrenia patients ($n = 34$) and MGH healthy controls ($n = 23$). After correction for multiple comparisons at the cluster level using Monte-Carlo simulation, there were negative associations between tract-specific FA in 5 WM tracts and 16 cortical brain regions in HCs (see online [supplementary material 2.1](#); [figures 1 and 2](#); [table 2](#) for cluster-wise P -values). There were no positive associations between FA and CT in controls and there were no significant associations between FA and CT in the group of SCZ patients. When controlling for multiple comparisons at the level of the 6 different tracts using Bonferroni

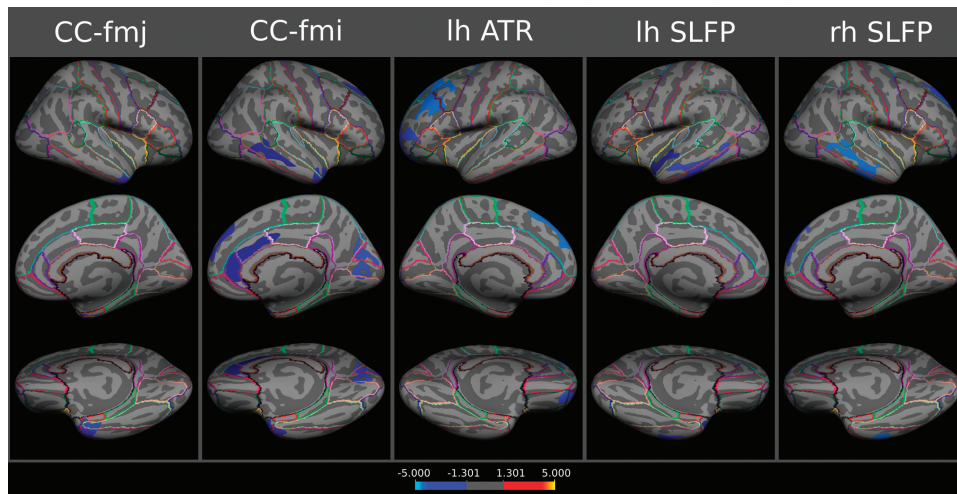


Fig. 1. Cortical statistical maps displaying negative associations between tract-specific fractional anisotropy and cortical thickness in healthy controls (mapped onto the surface of the FreeSurfer average brain). Cluster-wise probability values (corrected for multiple comparisons) are represented according to the color code and are all <0.05 . Abbreviations: lh, left hemisphere; rh, right hemisphere; SLFP, superior longitudinal fasciculus–parietofrontal part; ATR, anterior thalamic radiation; CC-fmj, corpus callosum forceps major, and CC-fmi, minor. For color version, please see figure online.

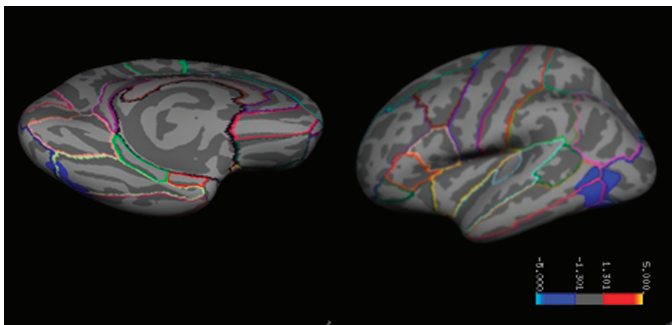


Fig. 2. Cortical maps displaying an association of the number of potholes with cortical thickness in schizophrenia patients (CWP = 0.00575; TalX, Y, Z = -39.8, -64.1, 3.4, respectively). For color version, please see figure online.

correction (ie, $P < .05/6 = 0.0083$), the following negative associations between CT and tract-specific FA in HCs remained significant: FA in the CC-fmj and CT in the rh temporal pole and inferior temporal gyrus; FA in the CC-fmi and CT in the cuneus; FA in the lh ATR and CT in the lh rostral and caudal middle frontal gyrus as well as lateral orbitofrontal cortex; FA in the lh SLFP and CT in the lh middle and inferior temporal gyrus as well as FA in the rh SLFP and CT in the rh middle and inferior temporal gyrus and superior frontal gyrus (labeled with an asterisk in [table 2](#); see also online [supplementary figure 3](#)). Some of these associations may be direct, ie, areas of reduced CT are locally adjacent to the endpoints of the WM tracts (see online [supplementary figure 4](#)).

When running the same GLM for the whole sample with diagnosis as a between-subject factor and the interaction between tract-specific FA and diagnosis, the negative association between FA in the lh ATR and CT

in the lh superior frontal gyrus was significantly larger in HC compared with the same in SCZ. Similarly, the negative association between FA in the rh-ATR and CT in the rh superior frontal and rh superior temporal gyrus was significantly larger in HC compared with SCZ (see online [supplementary table 2](#)).

Significant Associations Between White Matter Potholes and Cortical Thickness

Our cortex-wide analysis did not show any associations between the number of potholes and CT in HCs ($n = 130$). However, in SCZ patients ($n = 111$), the number of potholes correlated with reduced CT in the left inferior and medial temporal gyrus, left fusiform and left lateral occipital brain area ([figure 2](#)). For subanalyses regarding the effects of handedness and antipsychotic medication please refer to online [supplementary material 2.1](#).

Discussion

Using 2 very different forms of assessing WM characteristics and a well-validated analytic approach for measuring CT across the brain, we identified distinct associations between WM characteristics and regional thinning of the cortical ribbon. In HCs, FA in the corpus callosum, anterior thalamic radiation, and superior longitudinal fasciculus were negatively correlated with CT in associated brain regions, whereas this presumably normal relationship was disrupted in patients with SCZ. In contrast, WM potholes, ie, relatively large lesion-like regions with markedly reduced FA, were more prevalent in SCZ patients and associated with reduced thickness in temporal-occipital brain regions, specifically in patients.

Table 2. Associations Between Fractional Anisotropy in Manually Labeled White Matter Pathways and Cortical Thickness in Healthy Controls

Tract	Number of Cluster	Max	NVtxs	Size (mm ²)	TalX	TalY	TalZ	CWP	Annot
CC-fmj	1	-3.977	1880	1178.86	41.1	-5.2	-35.6	0.0055*	Inferior temporal
CC-fmi	1	-5.189	1682	1075.82	40.9	9.4	-32.3	0.012	Temporal pole
	2	-4.175	1852	882.06	7.4	32.5	11.4	0.0367	Rostral anterior cingulate
	3	-4.078	1562	865.81	64.1	-35	-5.9	0.0412	Middle temporal
	4	-3.598	1824	1342.34	16.5	-67.3	19.4	0.0025*	Cuneus
	5	-2.556	1621	964.1	13	40.3	38.1	0.0232	Superior frontal
lh ATR	1	-3.87	4931	2916.5	-28.6	29.5	32.3	0.0002*	Rostral middle frontal
	2	-3.337	1846	1373.21	-18.2	51.4	-14.7	0.0015*	Lateral orbitofrontal
lh SLFP	1	-5.662	1948	1236.76	-56.1	-28.7	-12.9	0.0037*	Middle temporal
	2	-2.295	1787	926.06	-33.5	13.3	-31	0.03	Temporal pole
rh SLFP	1	-3.471	1906	1160.88	15.6	42.6	34.8	0.003*	Superior frontal
	2	-3.465	2533	1446.04	64.1	-35.1	-5.5	0.0002*	Middle temporal

Note: NVtxs, number of vertices; TalX, Y, Z, Talairach coordinates; CWP, cluster-wise *P*-value; Annot, FreeSurfer annotation label.

*Association remains significant after controlling for multiple comparisons at the level of the 6 different tracts using Bonferroni correction ($P < .05/6 = 0.0083$).

Furthermore, we confirmed findings of previous studies, demonstrating reduced FA in a number of WM tracts,^{15,62,68,69} an increased number of WM potholes^{40,70} and substantially reduced CT in frontal, temporal, and occipito-parietal areas in patients with SCZ compared with HCs.^{25–28,64,66}

Increased WM integrity of specific WM tracts may be associated with improved global and local brain network connectivity and permit a more efficient organization of neuronal resources during normal development. In particular, superior connectivity might allow for appropriate synaptic plasticity, which could influence regional CT in healthy adults. In line with that, fMRI studies in healthy children suggest that developmental changes in patterns of brain activity involve a shift from diffuse to more focal activation, likely representing a fine-tuning of relevant neural systems with experience.⁷¹ Interestingly, GM thinning occurs at the same time and in the same locations as brain growth (particularly in the frontal lobe).⁷² However, the exact mechanism behind cortical thinning during normal development is not known. Cortical thinning during puberty has been associated with the loss of unneeded connections and synaptic pruning and may parallel a reduction in neuropil and glial cells.⁷³ Decreased GM and increased WM volume and integrity may also reflect progressive age-related myelin coating of fibers,⁷⁴ which is also assumed to occur in the lower cortical layers.³⁷ It is interesting to note that both greater cortical thinning and increasingly dense and ordered WM fiber tracts have also been associated with improved cognitive performance.^{72,75}

Negative relationships between WM integrity and GM characteristics have been observed previously.^{2,3} Giorgio et al (2008)² were one of the first to report that the age-related decrease in GM density in the right lateral prefrontal cortex correlates with FA increases in the superior

region of the corona radiata in healthy adolescents and young adults. Based on this negative association, they suggested that age-related changes may be occurring simultaneously in cortical GM and WM microstructure and that these changes may be a consequence of experience- and use-dependent regional development.^{73,76} More recent results by Tamnes et al (2010)³ support this conclusion. They also found significant, although somewhat weaker, negative correlations between CT in a large number of brain regions and FA in underlying tracts in healthy children, adolescents, and adults. These adaptive mechanisms, shaping neural circuits and thus providing a biological basis for ongoing development of cognitive abilities and behavior,⁷⁷ might be impaired in SCZ. The lack of the seemingly typical relationship between cortical GM and WM microstructure could be the morphological correlate of this disturbance.

In addition to the disturbance of general developmental mechanisms, there is evidence for more dramatic local WM disruptions such as potholes. “Potholes” as defined in this study represent relatively drastic disruptions in WM integrity that may occur at different “points of weakness” in different individuals and are unlikely to be associated with normative development. Early onset as well as typical adult SCZ patients have been shown to carry a higher load of potholes compared with HCs.^{40,41} Given the lesion-like nature of potholes, it is not surprising that the amount of potholes correlates with reduced CT in SCZ patients. These results are in line with the existing evidence for a dysconnectivity syndrome in SCZ. To date, the underlying biology of potholes remains to be clarified but possible reasons are related to inflammation,^{78,79} microvascular changes,⁷⁹ or oligodendrocyte pathology.

A recent study in SCZ patients and HCs corroborates our pothole findings.¹ In this study, the authors followed

up on an earlier finding in the same cohort demonstrating drastically increased radial diffusivity in an area of the left temporal cortex most probably containing fibers from the inferior and superior longitudinal fasciculus.⁸⁰ They found an association with decreased CT in the posterior cingulate cortex in patients, but not in controls. The markedly increased radial diffusivity in the WM region of interest (ROI) in patients in this study resembles our pothole definition and can be interpreted as resulting from demyelination or changes to the axonal cytoskeleton.⁸¹ Previous studies in patients suffering from multiple sclerosis came to complementary conclusions: Lesions in certain WM tracts seem to cause GM atrophy in connected regions via impaired axonal transport, anterograde, and retrograde degeneration of cell bodies or secondary neuronal loss.^{82–84} Similarly, the number of WM hyperintensities—which have a similar definition as potholes—have been researched extensively^{85–87} and have also been found to be associated with hippocampal atrophy in patients with Alzheimer disease.⁸⁸

Limitations

The present findings must be interpreted within the context of the study limitations. First, abnormal patterns of associations between WM characteristics and CT in SCZ patients may be influenced by the effects of antipsychotic medications. However, abnormal WM integrity and reduced cortical GM thickness have been shown to occur in persons with a high risk of developing SCZ and among neuroleptic-naïve and very young patients with a first episode of SCZ,^{89,90} implying the involvement of disturbed neurodevelopmental rather than pharmacological mechanisms. Furthermore, in our own (see online [supplementary Results](#)) and in the vast majority of previous studies^{8,41,91} cumulative antipsychotic exposure was not related to FA in any of the tracts studied or the number of potholes. When we covaried for cumulative antipsychotic exposure, the effect of WM potholes on CT in SCZ patients remained highly significant.

Second, due to the multisite study approach, our results could have been influenced by differences in MR scanner field strength and diffusion-weighted sequence acquisition parameters. However, it also provided increased statistical power, which enabled us to isolate relationships between WM potholes and CT in an unbiased manner, ie, without averaging across predefined a priori regions of interest. Furthermore, MRI findings that are platform independent (eg, independent of field strength or diffusion directions) would be more likely to be illness related. Several groups have studied the robustness of CT measurements using the same technology as in our study. Measurements across field strengths were found to be highly reliable⁹² and only slightly biased.⁹³ Similarly, the NORSA approach includes a standardization step within site and has been shown to produce relatively

consistent results across site.⁴¹ We covaried for the effects of acquisition site in all statistical models.

Third, a subanalysis comparing MCIC participants who were included in this analysis and participants who were excluded due to missing or low-quality brain imaging or other phenotype-related data revealed that excluded patients had higher positive, negative, and disorganized symptoms. Therefore, our findings may not apply to the most severely affected patients.

Finally, the interpretation of diffusion MRI studies is difficult due to our limited knowledge about the exact biological causes of diffusion anisotropy changes. Dividing WM tracts into subcomponents or using additional measures extracted from diffusion-weighted images, such as radial and axial diffusivity may help to identify underlying WM processes.⁹⁴ Changes in radial diffusivity have been found to accompany WM maturation in HCs,³ whereas axial diffusivity, the average magnitude of water molecule displacements parallel to WM pathways, is indicative of axonal health.^{95,96} In line with the developmental hypothesis, the associations between WM integrity and CT in our study (which we observed only in HCs) were driven by radial diffusivity (see online [supplementary table 4](#)).

Conclusions

In conclusion, this study revealed differential patterns of association between WM integrity and CT for HCs and SCZ patients. Although the pattern in HCs is characterized by slight decreases of CT with increasing FA and can be explained from a (normal) developmental perspective, reduced GM thickness in SCZ patients may be interpreted as the result of focal but spatially heterogeneous disruptions of WM integrity.

Supplementary Material

[Supplementary material](http://schizophreniabulletin.oxfordjournals.org) is available at <http://schizophreniabulletin.oxfordjournals.org>.

Funding

National Institutes of Health/National Center for Research Resources (P41RR14075); Department of Energy (DE-FG02-99ER62764); The Mind Research Network, Morphometry Biomedical Informatics Research Network (1U24, RR021382A); Function Biomedical Informatics Research Network (U24RR021992-01); National Institutes of Health/National Center for Research Resources (MO1 RR025758-01); Shared Instrumentation Grants (1S10RR023401, 1S10RR019307, and 1S10RR023043); National Institutes of Health (K99/R00EB008129 to A.Y.); National Institute of Mental Health (K08-MH068540 to T.W.); the NARSAD Young Investigator Award (to S.E.); Deutsche Forschungsgemeinschaft (to S.E.).

Acknowledgments

In the last 2 years, Dr Roessner has received lecture fees from Eli Lilly, Janssen-Cilag, Medice, Novartis and was a member of advisory boards of Eli Lilly, Novartis. All other authors declare that there are no conflicts of interest in relation to the subject of this study.

References

- Koch K, Schultz CC, Wagner G, et al. Disrupted white matter connectivity is associated with reduced cortical thickness in the cingulate cortex in schizophrenia. *Cortex*. 2012;49:722–729.
- Giorgio A, Watkins KE, Douaud G, et al. Changes in white matter microstructure during adolescence. *Neuroimage*. 2008;39:52–61.
- Tamnes CK, Ostby Y, Fjell AM, Westlye LT, Due-Tønnessen P, Walhovd KB. Brain maturation in adolescence and young adulthood: regional age-related changes in cortical thickness and white matter volume and microstructure. *Cereb Cortex*. 2010;20:534–548.
- Pierpaoli C, Basser PJ. Toward a quantitative assessment of diffusion anisotropy. *Magn Reson Med*. 1996;36:893–906.
- Basser PJ, Mattiello J, LeBihan D. MR diffusion tensor spectroscopy and imaging. *Biophys J*. 1994;66:259–267.
- Basser PJ, Mattiello J, LeBihan D. Estimation of the effective self-diffusion tensor from the NMR spin echo. *J Magn Reson Series B*. 1994;103:247–254.
- Basser PJ. Inferring microstructural features and the physiological state of tissues from diffusion-weighted images. *NMR Biomed*. 1995;8:333–344.
- Kyriakopoulos M, Bargiotas T, Barker GJ, Frangou S. Diffusion tensor imaging in schizophrenia. *Eur Psychiatr*. 2008;23:255–273.
- Kyriakopoulos M, Frangou S. Recent diffusion tensor imaging findings in early stages of schizophrenia. *Curr Opin Psychiatr*. 2009;22:168–176.
- Lawrie SM, McIntosh AM, Hall J, Owens DG, Johnstone EC. Brain structure and function changes during the development of schizophrenia: the evidence from studies of subjects at increased genetic risk. *Schizophr Bull*. 2008;34:330–340.
- White T, Nelson M, Lim KO. Diffusion tensor imaging in psychiatric disorders. *Top Magn Reson Imag*. 2008;19:97–109.
- Ellison-Wright I, Bullmore E. Meta-analysis of diffusion tensor imaging studies in schizophrenia. *Schizophr Res*. 2009;108:3–10.
- Buchsbaum MS, Friedman J, Buchsbaum BR, et al. Diffusion tensor imaging in schizophrenia. *Biol Psychiatr*. 2006;60:1181–1187.
- Andreasen NC, Flashman L, Flaum M, et al. Regional brain abnormalities in schizophrenia measured with magnetic resonance imaging. *JAMA*. 1994;272:1763–1769.
- Buchsbaum MS, Schoenkecht P, Torosjan Y, et al. Diffusion tensor imaging of frontal lobe white matter tracts in schizophrenia. *Ann Gen Psychiatr*. 2006;5:19.
- Crow TJ. Schizophrenia as a transcallosal misconnection syndrome. *Schizophr Res*. 1998;30:111–114.
- Karlsgodt KH, van Erp TG, Poldrack RA, Bearden CE, Nuechterlein KH, Cannon TD. Diffusion tensor imaging of the superior longitudinal fasciculus and working memory in recent-onset schizophrenia. *Biol Psychiatr*. 2008;63:512–518.
- Ostby Y, Tamnes CK, Fjell AM, Walhovd KB. Morphometry and connectivity of the fronto-parietal verbal working memory network in development. *Neuropsychologia*. 2011;49:3854–3862.
- Ehrlich S, Yendiki A, Greve DN, et al. Striatal function in relation to negative symptoms in schizophrenia. *Psychol Med*. 2011;1–16.
- Manoach DS, Gollub RL, Benson ES, et al. Schizophrenic subjects show aberrant fMRI activation of dorsolateral prefrontal cortex and basal ganglia during working memory performance. *Biol Psychiatr*. 2000;48:99–109.
- Honea R, Crow TJ, Passingham D, Mackay CE. Regional deficits in brain volume in schizophrenia: a meta-analysis of voxel-based morphometry studies. *Am J Psychiatr*. 2005;162:2233–2245.
- Segall JM, Turner JA, van Erp TG, et al. Voxel-based morphometric multisite collaborative study on schizophrenia. *Schizophr Bull*. 2009;35:82–95.
- Shenton ME, Dickey CC, Frumin M, McCarley RW. A review of MRI findings in schizophrenia. *Schizophr Res*. 2001;49:1–52.
- Wright IC, Rabe-Hesketh S, Woodruff PW, David AS, Murray RM, Bullmore ET. Meta-analysis of regional brain volumes in schizophrenia. *Am J Psychiatr*. 2000;157:16–25.
- Goldman AL, Pezawas L, Mattay VS, et al. Widespread reductions of cortical thickness in schizophrenia and spectrum disorders and evidence of heritability. *Arch Gen Psychiatr*. 2009;66:467–477.
- Nesvag R, Lawyer G, Varnas K, et al. Regional thinning of the cerebral cortex in schizophrenia: effects of diagnosis, age and antipsychotic medication. *Schizophr Res*. 2008;98:16–28.
- Schultz CC, Koch K, Wagner G, et al. Reduced cortical thickness in first episode schizophrenia. *Schizophr Res*. 2010;116:204–209.
- Ehrlich S, Brauns S, Yendiki A, et al. Associations of cortical thickness and cognition in healthy controls and patients with schizophrenia. *Schizophr Bull*. 2012;38:1050–1062.
- Gogtay N, Greenstein D, Lenane M, et al. Cortical brain development in nonpsychotic siblings of patients with childhood-onset schizophrenia. *Arch Gen Psychiatr*. 2007;64:772–780.
- Winkler AM, Kochunov P, Blangero J, et al. Cortical thickness or grey matter volume? The importance of selecting the phenotype for imaging genetics studies. *Neuroimage*. 2009;53:1135–1146.
- Hilgetag CC, Barbas H. Role of mechanical factors in the morphology of the primate cerebral cortex. *PLoS Computational Biology*. 2006;2:e22.
- Van Essen DC. A tension-based theory of morphogenesis and compact wiring in the central nervous system. *Nature*. 1997;385:313–318.
- Giedd JN, Blumenthal J, Jeffries NO, et al. Brain development during childhood and adolescence: a longitudinal MRI study. *Nat Neurosci*. 1999;2:861–863.
- Paus T, Zijdenbos A, Worsley K, et al. Structural maturation of neural pathways in children and adolescents: in vivo study. *Science*. 1999;283:1908–1911.
- Lebel C, Gee M, Camicioli R, Wieler M, Martin W, Beaulieu C. Diffusion tensor imaging of white matter tract evolution over the lifespan. *Neuroimage*. 2012;60:340–352.
- Beaulieu C. The basis of anisotropic water diffusion in the nervous system: a technical review. *NMR Biomed*. 2002;15:435–455.

37. Gogtay N, Giedd JN, Lusk L, et al. Dynamic mapping of human cortical development during childhood through early adulthood. *Proc Natl Acad Sci U S A*. 2004;101:8174–8179.
38. Sowell ER, Trauner DA, Gamst A, Jernigan TL. Development of cortical and subcortical brain structures in childhood and adolescence: a structural MRI study. *Dev Med Child Neurol*. 2002;44:4–16.
39. Brans RG, Kahn RS, Schnack HG, et al. Brain plasticity and intellectual ability are influenced by shared genes. *J Neurosci*. 2010;30:5519–5524.
40. White T, Schmidt M, Karatekin C. White matter ‘potholes’ in early-onset schizophrenia: a new approach to evaluate white matter microstructure using diffusion tensor imaging. *Psychiatry Res*. 2009;174:110–115.
41. White T, Ehrlich S, Ho BC, et al. Spatial characteristics of white matter abnormalities in schizophrenia [published online ahead of print September 16, 2012]. *Schizophr Bull*.
42. Ehrlich S, Morrow EM, Roffman JL, et al. The COMT Val108/158Met polymorphism and medial temporal lobe volumetry in patients with schizophrenia and healthy adults. *Neuroimage*. 2010;53:992–1000.
43. White T, Magnotta VA, Bockholt HJ, et al. Global white matter abnormalities in schizophrenia: a multisite diffusion tensor imaging study. *Schizophr Bull*. 2011;37:222–232.
44. First MB, Spitzer RL, Gibbon M, Williams JBW. *Structured Clinical Interview for DSM-IV-TR Axis I Disorders, Research Version, Nonpatient Edition*. New York: New York State Psychiatric Institute; 2002.
45. Andreasen NC, Flaum M, Arndt S. The Comprehensive Assessment of Symptoms and History (CASH). An instrument for assessing diagnosis and psychopathology. *Arch Gen Psychiatry*. 1992;49:615–623.
46. Wilkinson G. *Wide Range Achievement Test*. 3rd ed. Wilmington: Wide Range, Inc.; 1993.
47. Hollingshead A. *Two Factor Index of Social Position*. New Haven: Yale University; 1965.
48. Annett M. A classification of hand preference by association analysis. *Br J Psychol*. 1970;61:303–321.
49. Andreasen NC. *Scale for the Assessment of Positive Symptoms (SAPS)*. Iowa City: University of Iowa; 1984.
50. Andreasen NC. *Scale for the Assessment of Negative Symptoms (SANS)*. Iowa City: University of Iowa; 1983.
51. Andreasen NC. *Psychiatric Symptoms You Currently Have—Baseline (PSYCH-BASE)*. Iowa City, Iowa: The University of Iowa; 1987.
52. Jovicich J, Czanner S, Han X, et al. MRI-derived measurements of human subcortical, ventricular and intracranial brain volumes: reliability effects of scan sessions, acquisition sequences, data analyses, scanner upgrade, scanner vendors and field strengths. *Neuroimage*. 2009;46:177–192.
53. Jovicich J, Czanner S, Greve D, et al. Reliability in multi-site structural MRI studies: effects of gradient non-linearity correction on phantom and human data. *Neuroimage*. 2006;30:436–443.
54. Fischl B, Dale AM. Measuring the thickness of the human cerebral cortex from magnetic resonance images. *Proc Natl Acad Sci U S A*. 2000;97:11050–11055.
55. Fischl B, Sereno MI, Dale AM. Cortical surface-based analysis. II: Inflation, flattening, and a surface-based coordinate system. *Neuroimage*. 1999;9:195–207.
56. Fischl B, Sereno MI, Tootell RB, Dale AM. High-resolution intersubject averaging and a coordinate system for the cortical surface. *Hum Brain Mapp*. 1999;8:272–284.
57. Fischl B, Salat DH, Busa E, et al. Whole brain segmentation: automated labeling of neuroanatomical structures in the human brain. *Neuron*. 2002;33:341–355.
58. Desikan RS, Segonne F, Fischl B, et al. An automated labeling system for subdividing the human cerebral cortex on MRI scans into gyral based regions of interest. *Neuroimage*. 2006;31:968–980.
59. Buckner RL, Head D, Parker J, et al. A unified approach for morphometric and functional data analysis in young, old, and demented adults using automated atlas-based head size normalization: reliability and validation against manual measurement of total intracranial volume. *Neuroimage*. 2004;23:724–738.
60. Greve DN, Fischl B. Accurate and robust brain image alignment using boundary-based registration. *Neuroimage*. 2009;48:63–72.
61. Mori S, Crain BJ, Chacko VP, van Zijl PC. Three-dimensional tracking of axonal projections in the brain by magnetic resonance imaging. *Ann Neurol*. 1999;45:265–269.
62. Yendiki A, Panneck P, Srinivasan P, et al. Automated probabilistic reconstruction of white-matter pathways in health and disease using an atlas of the underlying anatomy. *Frontiers in Neuroinformatics*. 2011;5:23.
63. Wakana S, Jiang H, Nagae-Poetscher LM, van Zijl PC, Mori S. Fiber tract-based atlas of human white matter anatomy. *Radiology*. 2004;230:77–87.
64. Kuperberg GR, Broome MR, McGuire PK, et al. Regionally localized thinning of the cerebral cortex in schizophrenia. *Arch Gen Psychiatry*. 2003;60:878–888.
65. Walhovd KB, Fjell AM, Dale AM, et al. Regional cortical thickness matters in recall after months more than minutes. *Neuroimage*. 2006;31:1343–1351.
66. Narr KL, Bilder RM, Toga AW, et al. Mapping cortical thickness and gray matter concentration in first episode schizophrenia. *Cereb Cortex*. 2005;15:708–719.
67. Narr KL, Woods RP, Thompson PM, et al. Relationships between IQ and regional cortical gray matter thickness in healthy adults. *Cereb Cortex*. 2007;17:2163–2171.
68. Kubicki M, McCarley R, Westin CF, et al. A review of diffusion tensor imaging studies in schizophrenia. *J Psychiatr Res*. 2007;41:15–30.
69. Pettersson-Yeo W, Allen P, Benetti S, McGuire P, Mechelli A. Dysconnectivity in schizophrenia: where are we now? *Neurosci Biobehav Rev*. 2011;35:1110–1124.
70. White DA, Connor LT, Nardos B, et al. Age-related decline in the microstructural integrity of white matter in children with early- and continuously-treated PKU: a DTI study of the corpus callosum. *Mol Genet Metab*. 2010;99(Suppl 1):S41–S46.
71. Durston S, Casey BJ. What have we learned about cognitive development from neuroimaging? *Neuropsychologia*. 2006;44:2149–2157.
72. Sowell ER, Thompson PM, Leonard CM, Welcome SE, Kan E, Toga AW. Longitudinal mapping of cortical thickness and brain growth in normal children. *J Neurosci*. 2004;24:8223–8231.
73. Huttenlocher PR, Dabholkar AS. Regional differences in synaptogenesis in human cerebral cortex. *J Comp Neurol*. 1997;387:167–178.
74. Benes FM, Turtle M, Khan Y, Farol P. Myelination of a key relay zone in the hippocampal formation occurs in the human brain during childhood, adolescence, and adulthood. *Arch Gen Psychiatr*. 1994;51:477–484.

75. Schmithorst VJ, Wilke M, Dardzinski BJ, Holland SK. Cognitive functions correlate with white matter architecture in a normal pediatric population: a diffusion tensor MRI study. *Hum Brain Mapp.* 2005;26:139–147.
76. Bourgeois JP, Rakic P. Changes of synaptic density in the primary visual cortex of the macaque monkey from fetal to adult stage. *J Neurosci.* 1993;13:2801–2820.
77. Knudsen EI. Sensitive periods in the development of the brain and behavior. *J Cogn Neurosci.* 2004;16:1412–1425.
78. Fan JB, Zhang CS, Gu NF, et al. Catechol-O-methyltransferase gene Val/Met functional polymorphism and risk of schizophrenia: a large-scale association study plus meta-analysis. *Biol Psychiatry.* 2005;57:139–144.
79. Hanson DR, Gottesman II. Theories of schizophrenia: a genetic-inflammatory-vascular synthesis. *BMC Med Genet.* 2005;6:7.
80. Koch K, Wagner G, Schachtzabel C, et al. Neural activation and radial diffusivity in schizophrenia: combined fMRI and diffusion tensor imaging study. *Br J Psychiatr.* 2011;198:223–229.
81. Seal ML, Yucel M, Fornito A, et al. Abnormal white matter microstructure in schizophrenia: a voxelwise analysis of axial and radial diffusivity. *Schizophr Res.* 2008;101:106–110.
82. Bodini B, Khaleeli Z, Cercignani M, Miller DH, Thompson AJ, Ciccarelli O. Exploring the relationship between white matter and gray matter damage in early primary progressive multiple sclerosis: an in vivo study with TBSS and VBM. *Hum Brain Mapp.* 2009;30:2852–2861.
83. Sepulcre J, Goni J, Masdeu JC, et al. Contribution of white matter lesions to gray matter atrophy in multiple sclerosis: evidence from voxel-based analysis of T1 lesions in the visual pathway. *Arch Neurol.* 2009;66:173–179.
84. Perry VH, Anthony DC. Axon damage and repair in multiple sclerosis. *Philos Trans R Soc Lond B Biol Sci.* 1999;354:1641–1647.
85. Ehrlich S, Breeze JL, Hesdorffer DC, et al. White matter hyperintensities and their association with suicidality in depressed young adults. *J Affect Disord.* 2005;86:281–287.
86. Pompili M, Serafini G, Innamorati M, et al. White matter hyperintensities, suicide risk and late-onset affective disorders: an overview of the current literature. *La Clinica Terapeutica.* 2010;161:555–563.
87. Assareh A, Mather KA, Schofield PR, Kwok JB, Sachdev PS. The genetics of white matter lesions. *CNS Neuroscience and Therapeutics.* 2011;17:525–540.
88. de Leeuw FE, Barkhof F, Scheltens P. White matter lesions and hippocampal atrophy in Alzheimer's disease. *Neurology.* 2004;62:310–312.
89. White T, Andreasen NC, Nopoulos P, Magnotta V. Gyrfication abnormalities in childhood- and adolescent-onset schizophrenia. *Biol Psychiatry.* 2003;54:418–426.
90. Pantelis C, Velakoulis D, Wood SJ, et al. Neuroimaging and emerging psychotic disorders: the Melbourne ultra-high risk studies. *Int Rev Psychiatry.* 2007;19:371–381.
91. Whitford TJ, Kubicki M, Schneiderman JS, et al. Corpus callosum abnormalities and their association with psychotic symptoms in patients with schizophrenia. *Biol Psychiatry.* 2010;68:70–77.
92. Dickerson BC, Fenstermacher E, Salat DH, et al. Detection of cortical thickness correlates of cognitive performance: reliability across MRI scan sessions, scanners, and field strengths. *Neuroimage.* 2008;39:10–18.
93. Han X, Jovicich J, Salat D, et al. Reliability of MRI-derived measurements of human cerebral cortical thickness: the effects of field strength, scanner upgrade and manufacturer. *Neuroimage.* 2006;32:180–194.
94. Wozniak JR, Lim KO. Advances in white matter imaging: a review of in vivo magnetic resonance methodologies and their applicability to the study of development and aging. *Neurosci Biobehav Rev.* 2006;30:762–774.
95. Song SK, Sun SW, Ju WK, Lin SJ, Cross AH, Neufeld AH. Diffusion tensor imaging detects and differentiates axon and myelin degeneration in mouse optic nerve after retinal ischemia. *Neuroimage.* 2003;20:1714–1722.
96. Song SK, Sun SW, Ramsbottom MJ, Chang C, Russell J, Cross AH. Dysmyelination revealed through MRI as increased radial (but unchanged axial) diffusion of water. *Neuroimage.* 2002;17:1429–1436.